EUROPEAN COMMISSION

Community Research

Contract no.: 248231

MOSARIM

D2.2 - GENERATION OF AN INTERFERENCE SUSCEPTIBILITY MODEL FOR THE DIFFERENT RADAR PRINCIPLES

Report type	Deliverable
Work Group	WP2
Dissemination level	Public
Version number	Version 1.1
Date	2011-02-28
Lead Partner	Karlsruhe Institute of Technology
Project Coordinator	Dr. Martin Kunert

Dr. Martin Kunert
Robert Bosch GmbH
Daimler Strasse 6
71229 Leonberg
Phone +49 (0)711 811 37468
martin.kunert2@de.bosch.com

MOSARIM

SEVENTH FRAMEWORK PROGRAMME

Authors

Name	Company
Tom Schipper	Karlsruhe Institute of Technology
Andreas John	Hella KGaA Hueck & Co.
Martin Kunert	Robert Bosch GmbH

Revision chart and history log

Version	Date	Reason
0.1	2010-11-02	Initial version
0.2	2010-12-14	New radar model added
0.3	2011-01-03	Further graphics added, text modifications
0.4	2011-01-04	Text improvements
0.5	2011-02-03	Editorial and content improvements
0.9	2011-02-21	Text improvements, content improvements, structural improvements and finalizing for review process
1.0	2011-02-28	Reviewer comments implemented
1.1	2011-02-28	Final version for submission

SEVENTH FRAMEWORK PROGRAMME

Table of contents

Executive Summary

Within this report the problem how to assess the interference effects in a radar receiver is handled and first simulation demonstrations are given. A general document is created in parallel where informations about interference effects are collected during the further project work [GenDOC].

Interference in general describes the coherent superposition of two or more different waves at one point in space. A wave itself can be described as a rotating vector in the complex plane, where the addition of several vectors result in deterministic changes of magnitude and phase. The signal amplitude can be increased (constructive interference) or decreased (destructive interference).
Concretely, interference effects in automotive radar devices are caused by the superposition of disturbances from other radio devices (e.g. vehicular radar, surveillance radar, fixed links) at the receiving antenna with the incoming coherent use signals being reflected from objects within the radar's detection zone. These induced effects from other radar units in near vicinity to the victim radar receiver are called mutual radar interference.

When investigating the influence of mutual interference, the most intuitive approach is simply to take the path loss into account and calculate the received power at the interfered radar. When knowing the distance from an interferer to the victim radar, also a relative phase change can be considered which allows the rebuilding of more detailed time domain receive signals based on simple dynamic channels (victim and interferer are moving). Also a higher number of interferers can be considered, as well as any kind of adequate receiver topology. Based on changing noise floors first assessments of the interference effects can be performed. Such calculations are suitable to understand the general interference behaviour between different signal modulation schemes.
These calculations are based on simplified channel models, which do not take into account deterministic multi path effects, shading or diffraction. The obvious step is now a fusion of a detailed, modular signal processing with deterministic and more realistic channel models. A further step is then to abstract the detailed signal processing to increase the possible number of simulations.

The combination of signal processing modelling, channel modelling and assessment of interference effects are combined in so called susceptibility models. The task of the susceptibility models is to make interference effects visible.
Several possibilities for susceptibility models are introduced in this report and at least two of them should be considered in more depth during the project.

This report gives information about

- <u>The mainly considered radar topology</u>
  Here a topology is chosen that is suitable for systems based on CW, FSK, FMCW, FSK+FMCW and Pulsed+FMCW. More details about these radar topologies can be found in [1a,1b]

- <u>The expected interference effects along the functional blocks of the radar topology</u>
  Here a table is given which includes the important steps in the radars signal chain, started with the receiving antenna in order to understand the role of each function block in the occurring of interference effects.

- The different susceptibility models
  In general there exist three groups of susceptibility models.

  Numeric models are based on time time step-by-time step in order to match real world conditions/measurements.

  Analytic models replace the time step-by-time step simulations or channel simulations by a-priori knowledge in order to reach high computation speeds.

  Mixed models try to combine the benefits from both numeric models and analytic models

- The actual development status of the wave propagation simulation
  Here the used wave propagation simulation tool is introduced in more detail

- The actual development status of the post processing in Matlab
  Here the development status of the Matlab post-processing is introduced in more detail

Further, an example of an applied susceptibility model is given at the end of this deliverable.

Because this is a growing task the quality of the susceptibility models and the simulations will be continuously increased.

1. INTRODUCTION

The goal of simulations in the context of the MOSARIM project is to model and analyse interference effects by starting with very simplified assumptions and end up with complex and rather realistic scenarios. The outcome of all these simulation results in a better understanding how interference affects a radar victim receiver (susceptibility modelling) and how it is related to the traffic environment/density and the present modulation schemes used by all involved radars.

The basic simulation approach with its subdivision into a ray-tracing simulation part of the geometric scenario and a victim receiver signal processing part together with two alternative interfaces was already described in Task 2.1. [MT21]

Furthermore, in the initial project Tasks 1.3, 1.7 and 4.1 [D13, D17, D41], the two rather general interference effects “increased noise” and “occurrence of ghost targets” have been considered. But for a better in-depth understanding, a more detailed view and thus a simulation refinement is required. This is the main scope of Task 2.2.

In chapter 2, a more detailed consideration of system parts and possible interference effects is done. Based on these considerations, in chapter 3, different possible susceptibility models are derived and then presented in state-of-the-art and newly developed model details.
Examples regarding the degree reached within this task are presented in chapter 6 and a conclusion and outlook is finally given in chapter 7.

2. Detailed system considerations

2.1. Generic radar system topologies

In Task 1.3, for radar systems with different modulation schemes the respective receiver topologies are compiled. As it turned out, these can be traced back to two basic topologies, for pulse and for frequency-modulated radars, where only the topology for CW, FSK, FMCW, FSK+FMCW/LMFSK, Pulsed+FMCW is regarded in more detail (see Fig. 2.1). Pulse radars are not considered as victims, because they don't play an important role in current automotive radar systems due to their limited liability of mutual interference (pulse radars use amplitude information) and their own interference potential on other radars.

For the receiver topology in Fig. 2.1, that is described in detail in section 2.2, the propagation of interference effects along the signal processing chain is described.

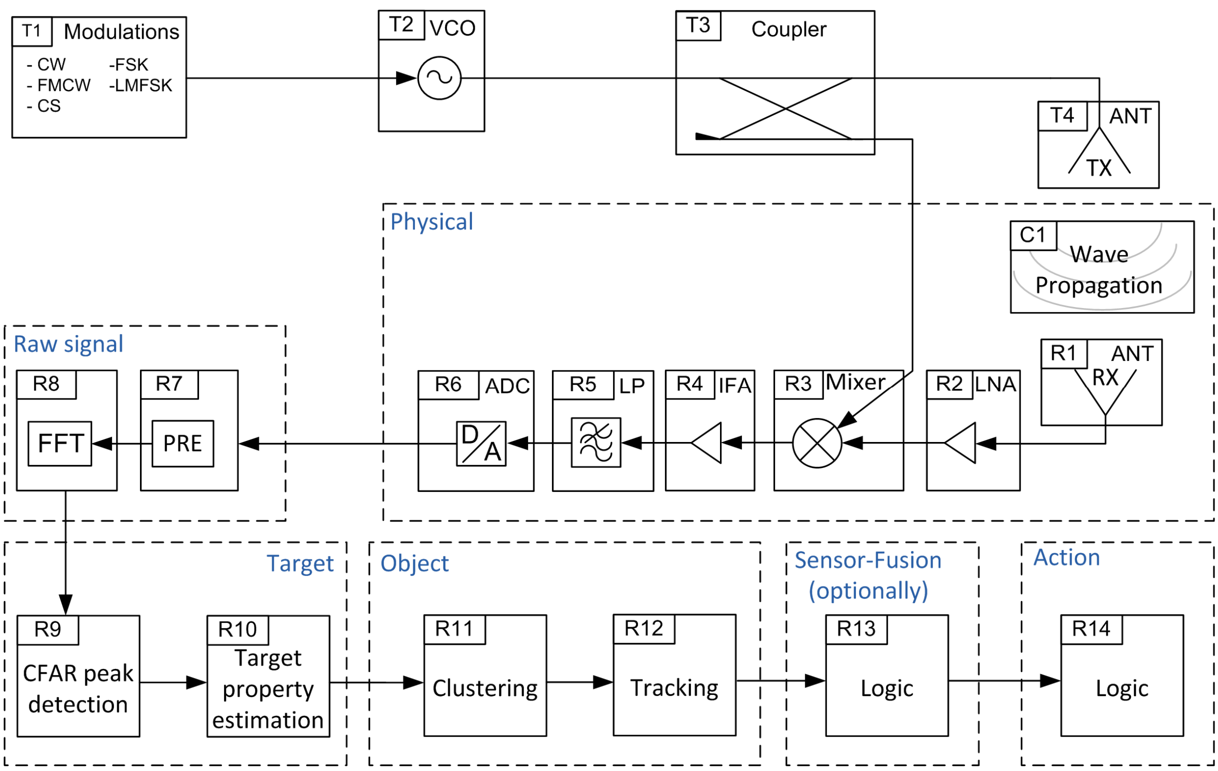

Fig. 2.1: System topology for CW, FSK, FMCW, FSK+FMCW and Pulsed+FMCW

2.2. Interference effects for CW, FSK, FMCW, FSK+FMCW, Pulse+FMCW

Considering the detailed generic system topology of Fig. 2.1, distortion of the analog and digital signal processing can theoretically occur according to Tab. 2.1

Layer	Receiver Elements	No.	Possible incident	Qualitative interference effect	Result for total sensor
Physical	Channel	C1.1	Multipath effects		
	Antenna	R1.1			
	LNA	R2.1	Driven into compression	Nonlinear distortion	
		R2.2	Driven into saturation	Clipping	
	Mixer Output	R3.1	Driven into compression	Nonlinear distortion	
		R3.2	Driven into saturation	Clipping	
	IFA	R4.1	Driven into compression	Nonlinear distortion	
		R4.2	Driven into saturation	Clipping	
	Active IF filter output	R5.1	Interference with "short" dwell time	Parasitic timely "short" overlayed signal	See R8.1
		R5.2	Interference with "long" dwell time	Parasitic periodic overlayed signal	See R8.2
		R5.3	Driven to max. supply voltage	Clipping	
	ADC output	R6.1	Driven to max. numeric value	Clipping	
Raw signal	Prefiltering	R7.1			
	FFT result	R8.1	See R5.1	Increased noise	Reduced sensitivity and thus reduced range

		R8.2	See R5.2	Single or multiple parasitic peaks	Danger of single or multiple ghost targets
Target	CFAR peak detection (target detection)	R9.1	See R8.1 and R8.2	Increase of adaptive detection level	Reduced sensitivity and thus reduced range
		R9.2	See R8.2	Parasitic peaks	Ghost targets, reduced sensitivity
	Target property estimation	R10.1		Not yet implemented	Not yet implemented
Object	Clustering (object detection)	R11.1		Not yet implemented	Not yet implemented
	Object tracking	R12.1		Not yet implemented	Not yet implemented
Sensor-Fusion	Logic	R13.1		Not yet implemented	Not yet implemented
Action	Logic	R14.1		Not yet implemented	Not yet implemented
				Not yet implemented	Not yet implemented

Tab.2.1: Theoretical distortions inside the analog and digital signal processing chain (make the formats for tables and figures description consistent over whole document)

Quantitatively, interference effects differ from sensor model to sensor model because different suppliers use different hardware implementations and different software algorithms.

3. Development of susceptibility models

3.1. Numeric and analytical models

In general there exist several approaches to build up a susceptibility model. (In this document it will be referred as M1.)

Models based on channel impulse responses and detailed, generic radar systems are one possible solution. These models are called "numeric" in this document. They enable a reconstruction of interference effects and their interpretation with a higher level of detail. Extracted noise floors and, if peak detection is also implemented, the occurrence of ghost targets can be used for the interference assessment. This approach has the drawback of a noticeable simulation time.

The other modelling approach is the implementation of "analytic" susceptibility models (in this document it will be referred as M2). These approaches reduce the simulation effort in comparison to the detailed models mentioned before by replacing the time step-by-time step signal creation of the numeric model with a-priori knowledge of the interaction behaviour of the modulation schemes in the IF-frequency band. Dependent on the degree of abstraction, even the wave propagation simulation could be replaced by applying the radar equation and assuming a **R**adar **C**ross **S**ection (RCS) for a target, if a certain scenario conditions should be checked due to its reliability.
Important is, that all kind of abstractions make the calculation of the interference probability more feasible by reducing the amount of computation power needed.

Both the analytical and numerical susceptibility model extremes are sketched in Fig. 3.1.

In comparison to interference effect studies conducted in European Electronic Communications Committee [CEPT] the simulation models within the MOSARIM project are based on deterministic channel data and include 3D wave propagation simulations.

Fully numeric model (M1)

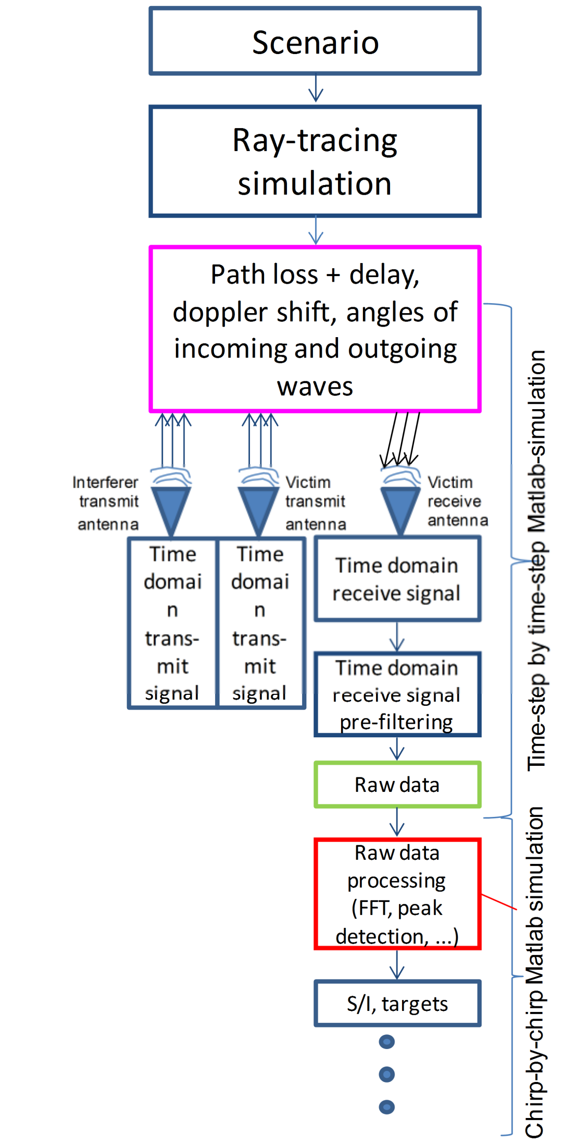

Fully analytic model (M2)

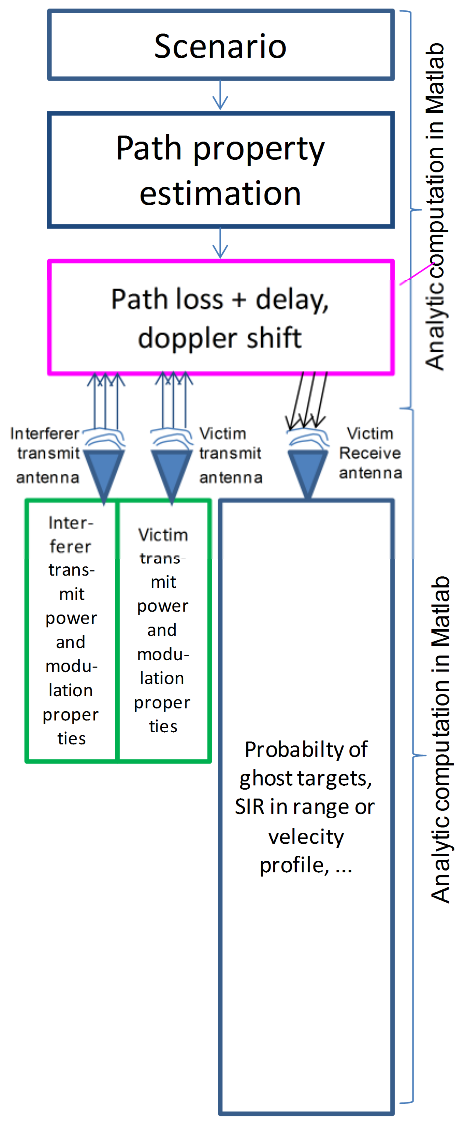

Fig. 3.1: Visualization of the fully numerical and analytical susceptibility model

3.2. Mixed models

The *"mixed"* models presented next try to combine a faster computation of the modulation schemes' interaction behaviour with more detailed, calculation-intensive sections that are still simulated in the time domain. (Fig. 3.2)
Susceptibility model M5 is of special interest because only the victim radar's own signals are considered in more detail in the time domain, whereas all other interferer-contributions are considered abstractly to reduce the amount of computational effort.

A realization of the susceptibility model M4 uses detailed knowledge about the interaction behaviour between the different modulation schemes and delivers the probability of interference while still considering the deterministic channel simulation by ray-tracing. This model needs the most advanced analytic researches.

The idea of the susceptibility model M3 is to speed up the Model M1. By describing a signal by its frequency slopes, sweep lengths (FMCW,CS), step sizes, step lengths (FSK,LMFSK) and its transmit powers the signals have not to be described in the time domain any more. But a normal signal processing after the FFT is still possible, where M4 does not provide this possibility.

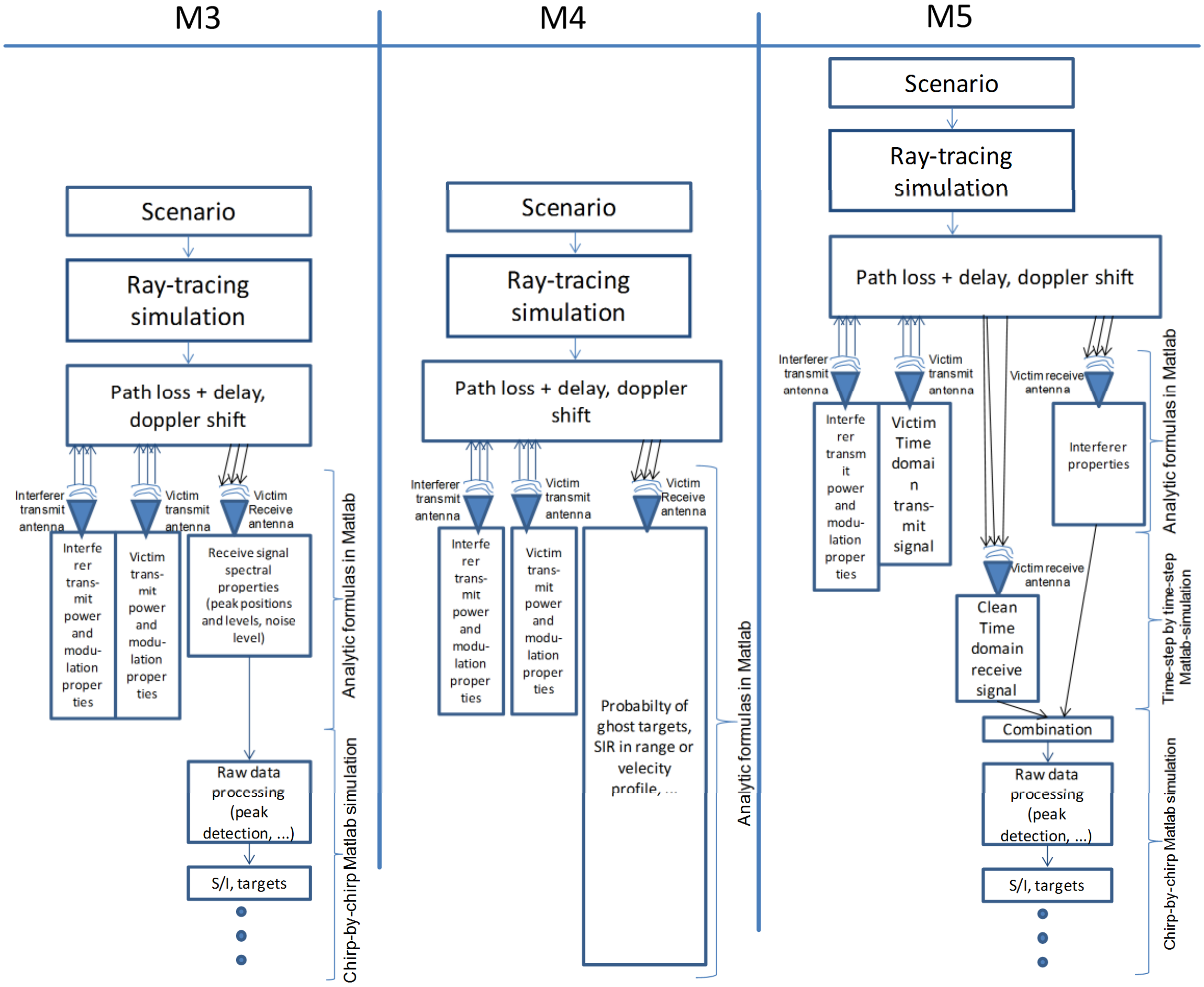

Fig. 3.2: Visualization of three mixed numeric/analytic susceptibility models

3.3. Initially selected models

The most suitable susceptibility models will be figured out during the further project work while further developing the simulation chain. For now, two susceptibility models will be further considered:

a) The fully numeric approach M1 (for controlling the correctness of the overall simulation approach and to verify measurement data from task 4.1, *"Ground truth interference assessment"*)

b) Model M3 should enable the step towards a higher number of simulations while a further signal processing is still possible. The higher number of simulation should enable probability considerations.

Fig. 3.3 and 3.4 show the two considered models in a more detailed way including the possibility of an interference assessment based on automated comparisons of real and detected object positions and velocities.

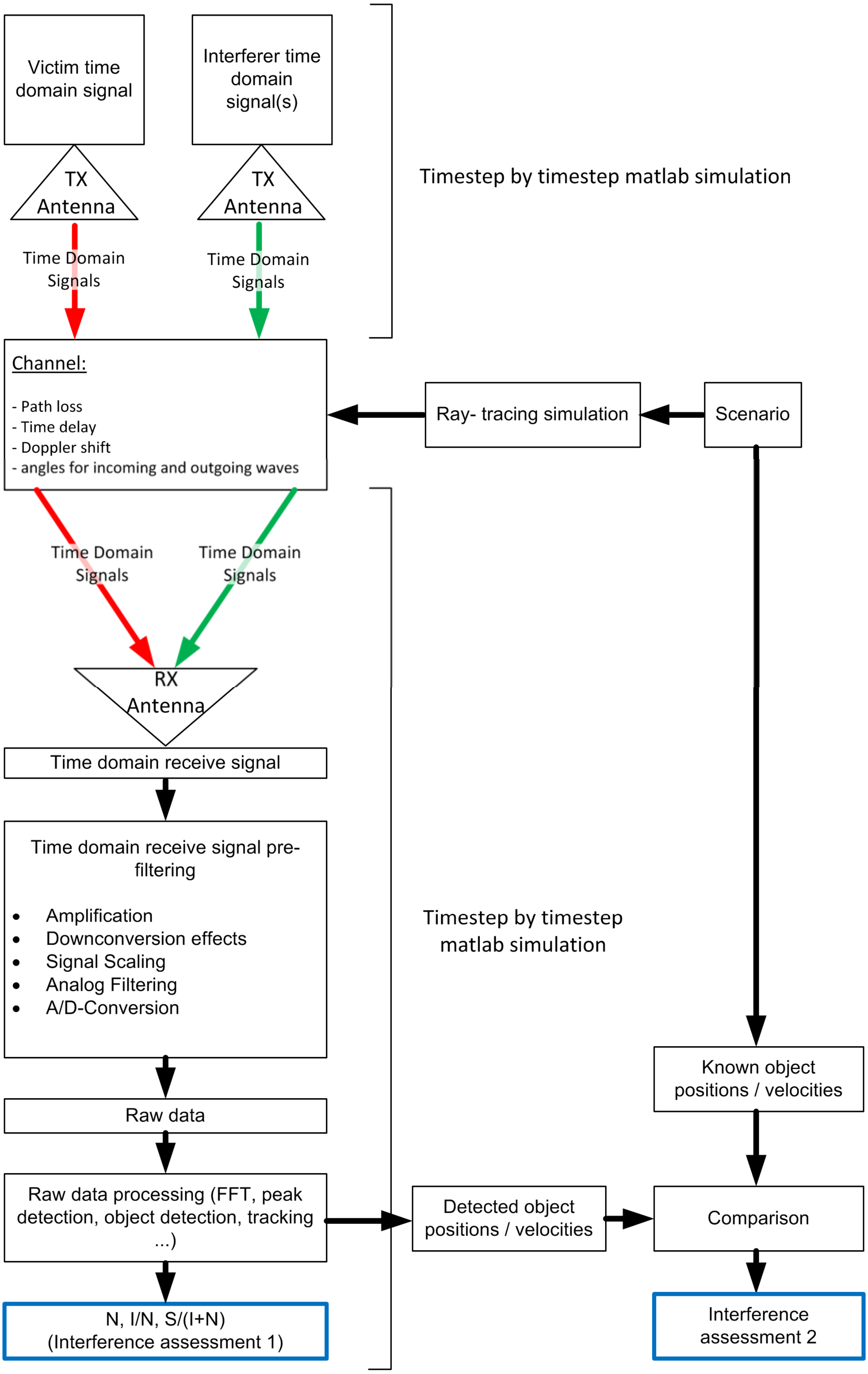

Fig. 3.3: Example of M1 realization

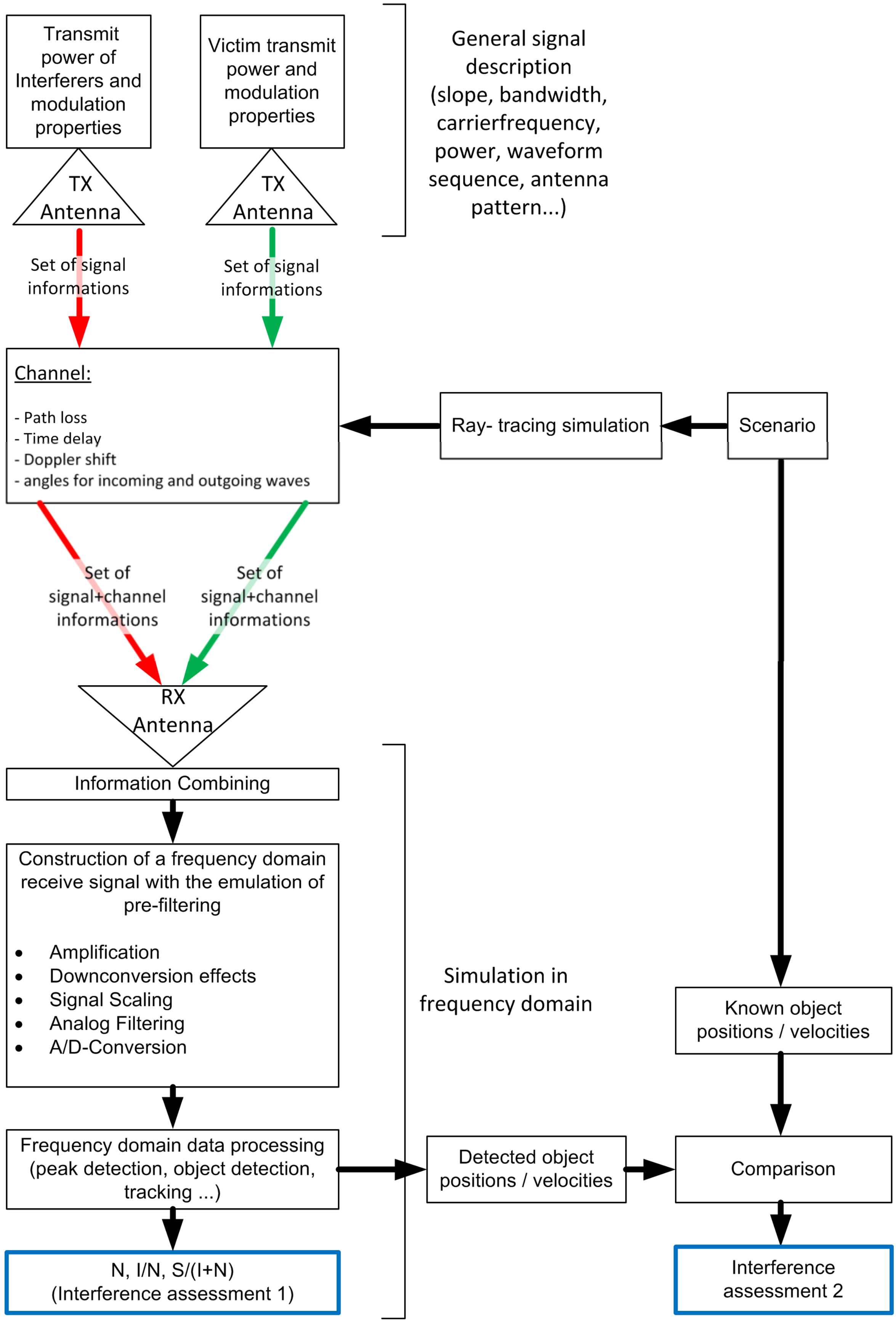

Figure 3.4: Example of M3 realization

Common for the two approaches in Figure 3.3 and 3.4 is the need for ray-tracing simulation. The current development state of this part is described in more detail in chapter 4.

The main differences between the two approaches occur in the Matlab signal processing part. The current development state of that part is described in more detail in chapter 5.

4. 3D ray-tracing simulation: state-of-the-art and new developments

4.1. Wave propagation modeling

The fully polarimetric wave propagation modeling is based on the common method of Geometrical-Optics (GO), i.e. a high frequency approximation which allows fast computation of large electromagnetic field problems [4a]. The model can handle reflections by considering modified Fresnel reflection coefficients which take into account a certain surface roughness that results in a causal decreased amplitude of the reflected wave [4b]. The **U**niform **T**heory of **D**iffraction (UTD) is also implemented to realize the diffraction behavior at wedges [4c]. It is possible to define Lambertian scattering sources, which are used to model vegetation [4d]. The ray-tracing tool calculates all possible propagation paths with respect to the mentioned propagation effects.

There are two things to be noted when using the GO for wave propagation simulations: The first one is that the use of the GO requires compromises regarding polygon sizes. If the size of the polygon is much larger than the wavelength, then the GO approximation provides a reliable estimation.

The second point is, that ray-tracing is not able to consider a structure's RCS, unlike for example **F**inite **D**ifference **T**ime **D**omain (FDTD) or **P**hysical **O**ptic (PO) techniques. Approaches exist which combine the speed of GO while considering proper backscattering behavior of objects by using look-up tables for scattering centers [4e].

For the simulation chain, arbitrary configurable scattering sources are currently developed to map certain target RCS behavior onto objects with only a few polygons to decrease computation time (see section 4.3). The normal GO shows that for perfect conducting materials a behavior for backscattered energy that decreases proportional with the distance by the power of 2, whereas energy scattered back by the arbitrary scattering sources decreases with the distance by the power of 4 (matches with the radar equation). This very primitive method to map RCS on an object is based on both measurement results and simulations.

4.2. Generation of the environment

A new map editor has been developed and improved and can be used in the further MOSARIM project work (Fig. 4.1). The map editor can import standard polygon structures in the common STL (**S**tandard **T**riangulation **L**anguage) format. It is possible to generate arbitrary scenarios and assign all simulation relevant parameters (ε', ε'', μ', μ'', σ for surface roughness, and parameters for Lambertian scatterers [4d]) to a polygon or a group of polygons. Also every object in the editor can have its own velocity vector. Due to that, the movement of all objects over time can be verified before starting the time consuming simulations. If all scenario requirements are met, the scenario is then exported and processed by the ray-tracing tool.

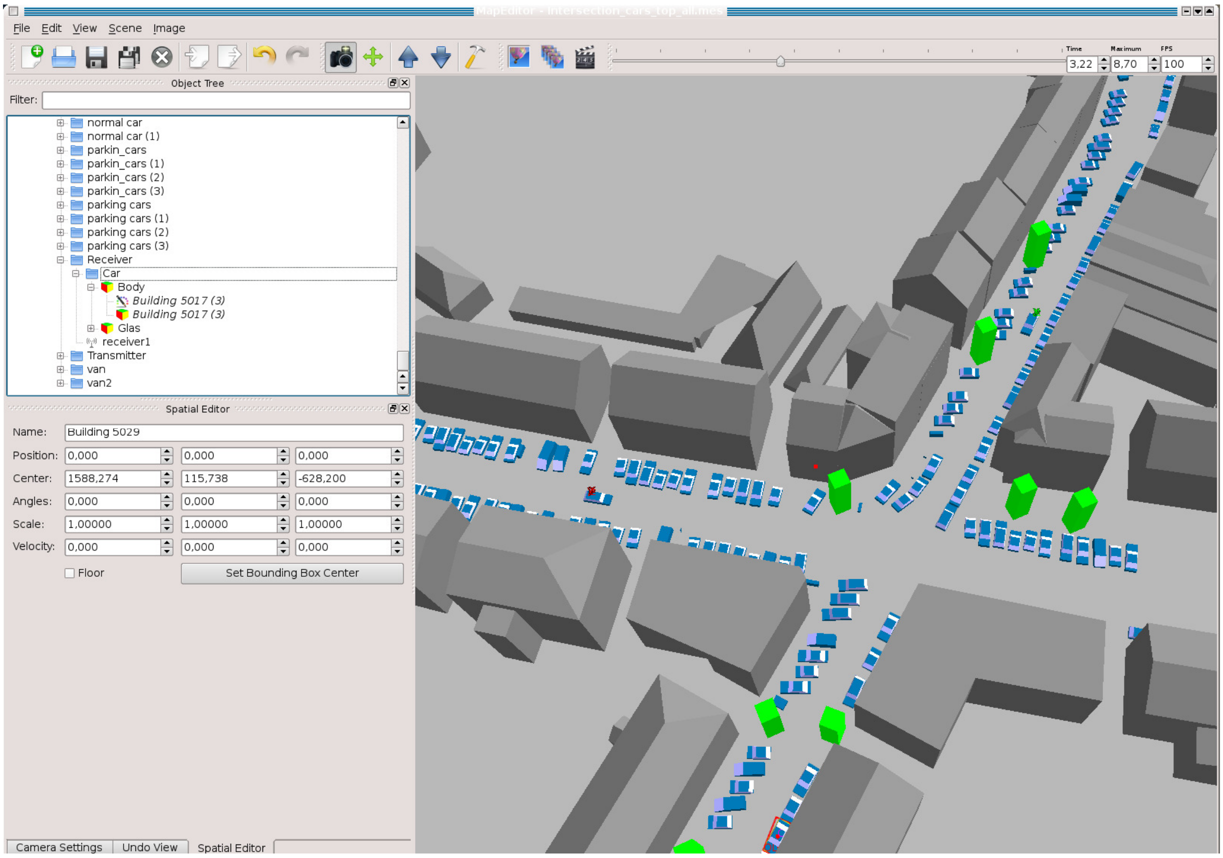

Fig. 4.1: Used map editor for scenario generation

4.3. Ray-tracing simulation

The ray-tracing algorithm inserts a user defined transmitter-receiver antenna combination and runs a simulation for every transmitter-receiver combination while using the wave propagation modeling which has been described in section 4.1. The ray-tracing tool uses, besides directly loaded **C**omputer **S**imulation **T**echnology [4f] or HFSS [4g] antenna patterns, dual polarized ideal omni-directional antennas.
The number of transmitters or receivers is not limited. The ray-tracing results provide the following data for every single propagation path: Amplitude and phase for all four transmitter-receiver polarization combinations, the propagation time of the path, a Doppler frequency shift and a path identification, which is unique and can be used to determine a path's lifetime, for example. All paths can be back-traced in order to find interaction points with the environment, what can be used for example for finding scattering centers [4h].
Every object in the scenarios to be simulated can have a certain velocity vector. This enables a comfortable reconstruction of the road traffic scenarios. With a couple of single simulations in a row time variant, dynamic simulations can be established.
The results for every separate transmitter-receiver combination can later be superimposed (e.g. for adding up all energy contributions of all radars in a scenario at the observing radar's receiver for interference assessments).

Typical effects which occur in real street scenarios are regarded in following way:

Multi-path effects: Are considered by ray-tracing method (mirror- or image-method).

Poles/Guardrails: Are considered by their reflection behavior. Their dimensions have to be bigger than 5-10 times the wavelength (=min 6.25 cm for 24 GHz radar and about 2 cm for 77 GHz radar). These values are based on empirical results.

Clutter from road: Clutter can be considered by using incoherent scattering parameters for the street in an extra simulation run for the victim radar. The clutter can later be superimposed with results from simulation runs with a normal road and coherent reflection.

Radar Cross Section: Can not be considered directly because the ray-tracing architecture is originally trimmed for communication. It is possible to model certain RCS behavior by scattering sources. See more details about RCS modeling in section 4.3.

Fig. 4.2 illustrates the ray-tracing simulation flow for a scenario with two interferers and one victim. Every transmitter – receiver combination is processed separately. In the first simulation run the transmitter/receiver for the victim receiver is considered. In further simulation runs the combination “interfering sensors – victim receiver” is considered.

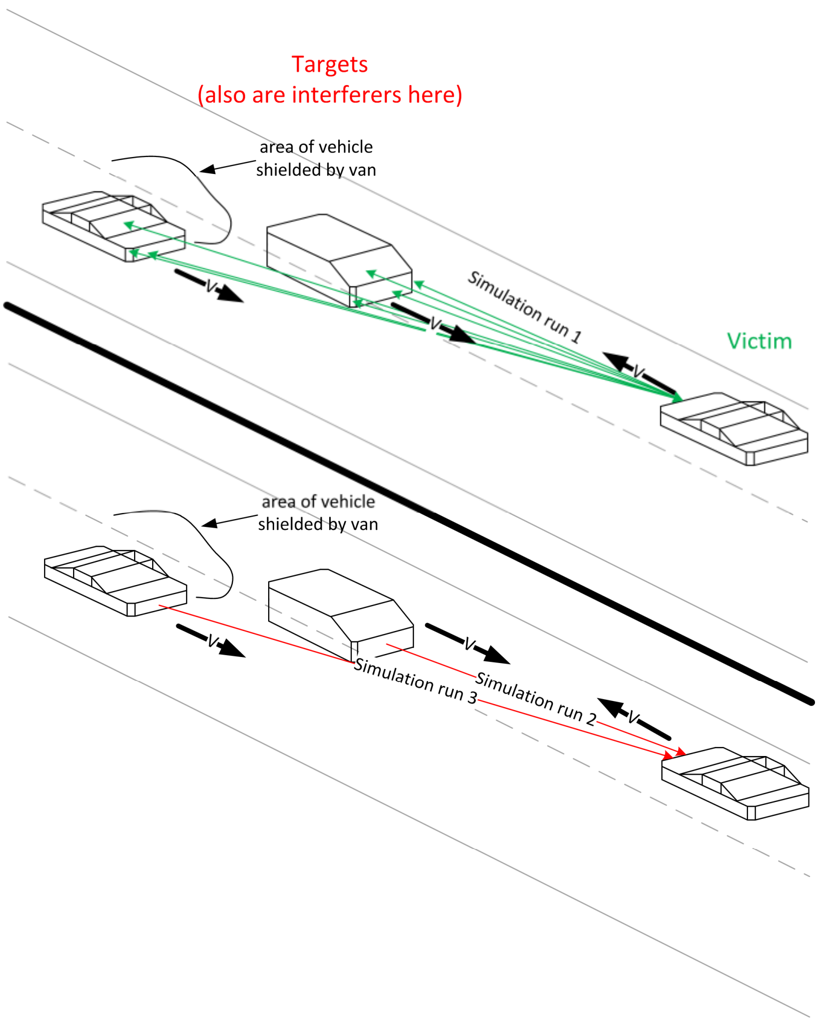

Figure 4.2: Principle of the ray-tracing simulation considering monostatic RCS for victim and multiple interfering devices with common GO wave propagation approach

4.4. Object and RCS modeling

Every single object to be processed by the ray-tracing algorithm is built of polygons. The objects can be imported from existing 3D CAD models (if they are in stl-format or can be converted into stl-format) or can be drawn by the user. The higher the number of polygons, the slower the simulation speed. Because it is dealt with a high number of simulations when observing dynamic scenarios (moving objects, high number of radar devices with different modulation schemes, high number of multi paths) the number of polygons should be kept as low as possible. But when the number of polygons is reduced, the probability for reflections decreases for monostatic radar scenarios due to the implemented mirror method for path finding. (Mirror method: the propagation paths are “traced” from source to sink where every interaction point is assumed to be very large in comparison to the wavelength. It is assumed that plane wave conditions are fulfilled. There is no ray relaunch for every interaction point with a polygon’s surface, so a direct back-reflected wave can only happen for an polygon which is oriented orthogonally towards the monostatic victim radar).

An important point, when the whole radar signal chain should be simulated deterministically, is the modeling of the target’s RCS. These RCS values have to match real measurements or simulated RCS values sufficiently in order to generate reliable use signals. It is especially important that different objects have suitable relative RCS values. That means that a car must have a large RCS in comparison to a pedestrian and a lorry must have a larger RCS than a car. A modeling approach based on modifiable Lambertian scattering sources has been started to make the generation of a RCS dependent use signal for monostatic radar scenarios possible.

Therefore monostatic RCS measurements were performed in ISPRA, Italy at the beginning of August 2010 on the objects listed in Tab. 4.1 (see example setup in Fig. 4.3). Some measurement results are shown in Fig. 4.4 and 4.5.

Object
Fiat Ducato van
Audi A4 estate
VW New Beetle I
VW Golf V
Scooter with mannequin
Bike
Mannequin

Table 4.1: Objects used for mono-static RCS measurements

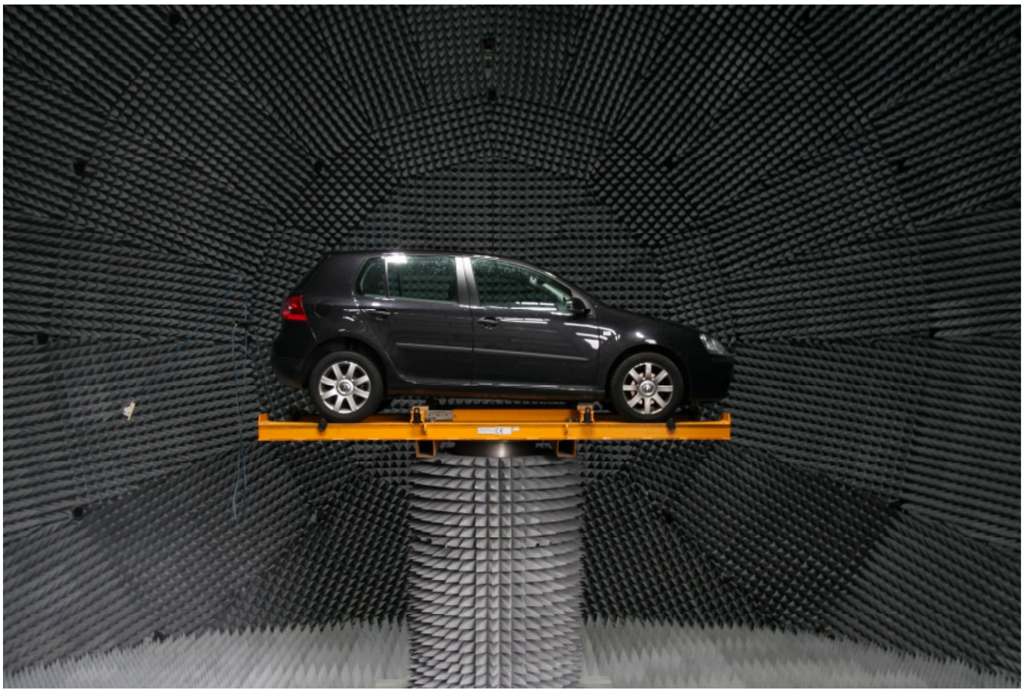

Figure 4.3: Example measurement setup with VW Golf V

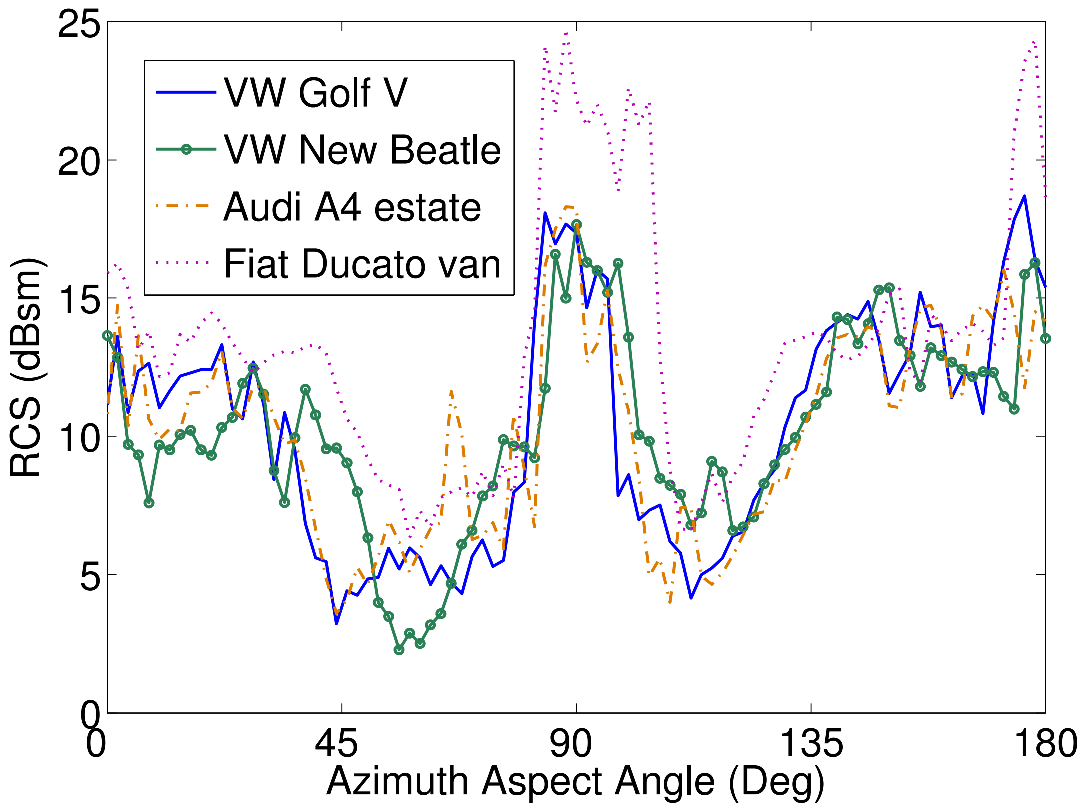

Figure 4.4: Mono-static RCS measurement for three vehicles at 24 GHz (0° azimuth means view to front of vehicle).

A first result for a compact car model, that should match the RCS of a Golf V is shown in Fig. 4.6. This result was achieved with 4 scattering centers, where the whole model has 14 polygons. The graph shows an ideal behaviour up to now, this should be handled by adding a deterministic phase distribution during the further project.

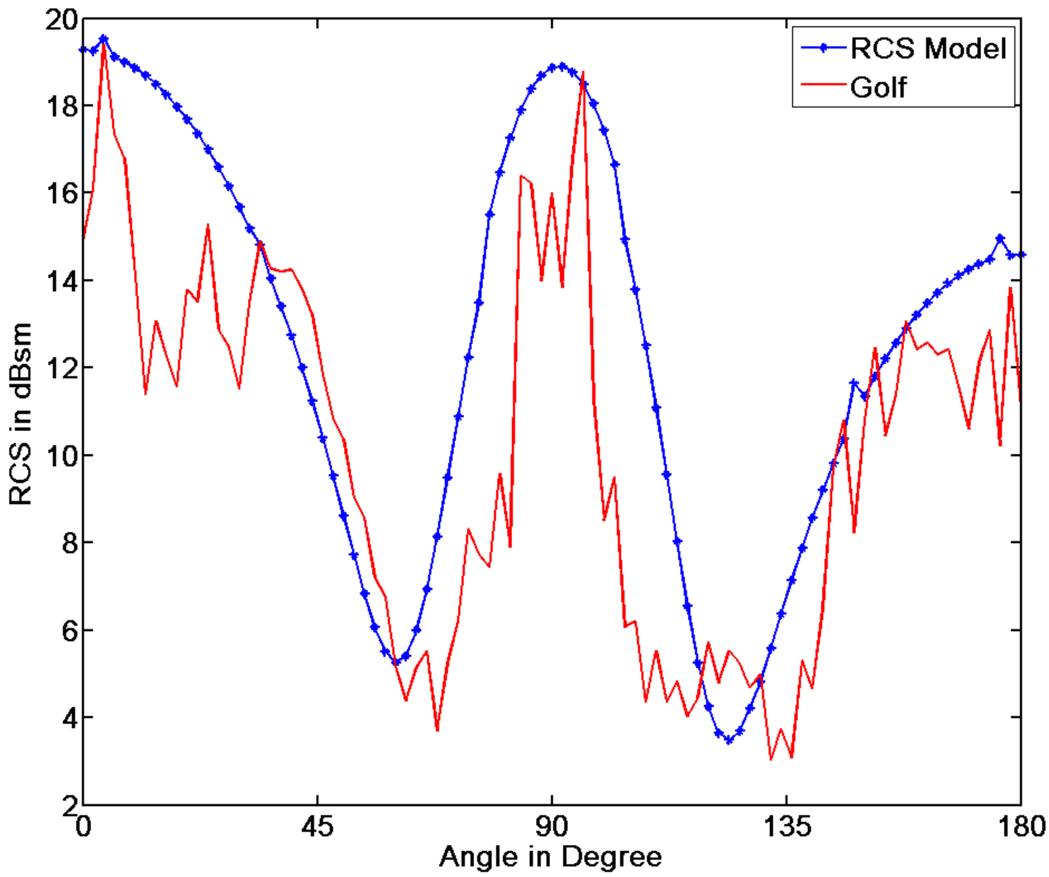

Fig. 4.5: Modeled RCS based on measurements gathered from Golf V (0° is view to the back of the vehicle)

5. Matlab signal processing: State-of-the-art and new developments

5.1. Fully numeric model

The first processing step is the generation of all involved transmit signals in the time domain by the reconstruction of real sensor transmit signals. Those generated transmit signals will be referred further as originally created signals.

In the next step the channel impulse responses, which are obtained by the ray-tracing simulations, are combined with the antenna patterns (loaded from data files). The result is an updated set of impulse responses which already includes the antenna effects.

Then the originally created signals are processed by using the channel impulse responses and the Doppler-frequency shifts. This gives time step-by-time step time domain victim receiver antenna input signals.

Next, the signal propagation through the hardware-based signal processing chain in the victim receiver part is considered. Here, different approaches exist to model for example filters or mixers:

- Analytic behavioral model
- Table-based model
- Equivalent circuit model

The current implementation uses simple ideal analytic models, which can be replaced later by more complex models, if necessary.

Finally, the software-based signal processing in the victim receiver part is considered. There exist different approaches:

- Doing numerical calculus without or with limited computational resources (like bit-length of a numeric value) normally found in a real DSP
- Using generic algorithms or using proprietary algorithms for raw-signal, target- and object-processing

The current implementation includes generic processing of raw data without limited computational resources up to the CFAR-threshold.

Generic target- and object-processing are planned to be included during the further project work.

5.2. Mixed numeric/analytic model

For *analytic* approaches the signals are represented by their modulation properties (slope, number and kind of frequency stepping, transmit power, repetition time …)

In the next step the channel impulse responses which are obtained by the ray-tracing simulations are combined with the antenna patterns (loaded from CST, HFSS or antennas created in Matlab). The result is an updated set of impulse responses which already include the antenna effects.

For *mixed numeric/analytic* susceptibility model approaches the information about the characteristics and interaction of different modulation schemes is used instead of detailed time step-by-time step transmit signals to reduce the computational effort. The goal is to get a good level of consistence with the *numeric* simulations. The analytic susceptibility models will allow to get probability values for the occurring of relevant interfering situations together with the grade of interference.

5.3. Details about the signal generation and processing

When realizing model M1, all time domain signals are generated as complex signals in the baseband because signals at 24 or 76 GHz would need to high sample rates. The sampling rate for the generated signals is at least

$$f_{sample} \geq 8 \cdot \left(f_{sweep} + \max\left(f_{doppler}\right)\right) \qquad \text{(f6a)}$$

where due to limited anti aliasing filter slopes the factor 8 is used in (f6a). Exactly one period of every signal sub-sequence is stored (a sub-sequence is, e.g., every single frequency ramp in an FMCW signal). The signal is sent over the channel in the following way while considering the path properties from the ray-tracing results. It is assumed that the antennas are already applied to the channel dataset. Every single path is processed for itself, due to the nonlinear behavior of the channel

1. Considering frequency shift

   $$\vec{s}_f = \vec{s} \cdot \exp(j 2\pi f \cdot \vec{t}) \qquad \text{(f6b)}$$

   where $\vec{s}$ is the signal to be transmitted and $\vec{t}$ is the time vector used for sampling the original signal.

2. Considering amplitude and phase

   $$\vec{s}_{f,A,\varphi} = \vec{s}_f \cdot A \cdot \exp\left(j\varphi\right) \qquad \text{(f6b)}$$

   where A is the amplitude and and φ is the phase.

3. Considering time shift

$$\vec{s}_{f,A,\phi,t} = circshift\left(\vec{s}_{f,A,\phi}, round\left[\frac{t_d}{t_s}\right]\right) \qquad \text{(Matlab pseudo code)} \qquad \text{(f6c)}$$

where t_d is the time delay of the path and t_s is the sampling time of the original signal.

After applying these steps, the signal is ideally amplified (no compression considered), casted to real signals and mixed with the originally sent signal. The resulting IF-signal is further amplified and a 4th order Butterworth low pass filter is applied. The signal is then downsampled with the sampling frequency f_a, and quantized with a resolution of e.g. 14bit, where the maximum operating voltage of the ADC is considered. The number of samples N is dependent on the length of the frequency ramp, T_{ramp}, which has to be sampled with the frequency f_a, and is equal to

$$N = T_{ramp} \cdot f_{sample} \qquad \text{(f6d)}$$

Then the signal is windowed and an FFT is applied. Further signal processing, like CFAR threshold, target detection and tracking are thinkable.

5.4. System noise

The noise contribution is modeled as additional white Gaussian noise directly at the place of incurrence.

Alternatively, the Friis formula could be used to generate the noise directly in the use bandwidth at the end of the analog signal chain.

6. Example results

In this chapter two examples of radar simulations are presented. The first example, described in section 6.1, visualizes the interference between a victim FMCW radar system and an interfering CW road speed meter. The effect is an *increasing noise floor* if frequency ramps with different slopes as the victim radar are received. The second example shows the *ghost target effect* resulting from multipath effects in a tunnel scenario.

6.1. Interference by a road speed meter

The model M1 – numerical (see section 3.3) is used to simulate an example scenario, where a FMCW radar interferes with a road speed meter (Fig. 6.1). The victim is a 24GHz FMCW Forward Looking Radar (FLR) which is interfered by a CW road speed meter (RSM). Detailed parameters for the victim and interferer can be found in Tab. 6.1.

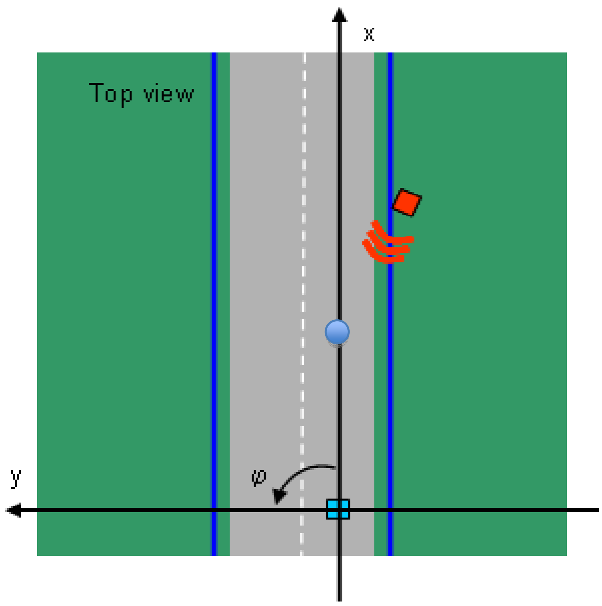

Fig.: 6.1: Visualisation of scenario used for comparison of the two susceptibility models.

Interferer position:
- x = 190m
- y = -4m
- z = 1.0m

FLR victim position :
- x = 140m
- y = 0m
- z = 0.4m

Synthetic target:
- x = 170m
- y = 0m
- z = 0.4m
- perfect reflector (only one path considered)

Road :
- width = 2 * 3.5m
- material = concrete

Guard rail positions :
- y = -2.5m, 6m
- height = 0.6m
- material = perfect conductor

Object	Parameters	Description
Victim: FLR at 24GHz	Transmitter	Radar principle: FMCW (type B3 according to [MT21]), FMCW parameters: • Transmit power = 20dBm eirp • Center frequency = 24.15GHz • Chirp span = 200MHz, • Chirp slope = 6 GHz/s,

		• Chirp duration = 33 ms • Chirp types: only Up-chirps: / / / Antenna characteristics: • 3dB azimuth width = +/- 10.0°, • 3dB elevation width = +/- 5.0°, • 1st side lobe = -20dBc 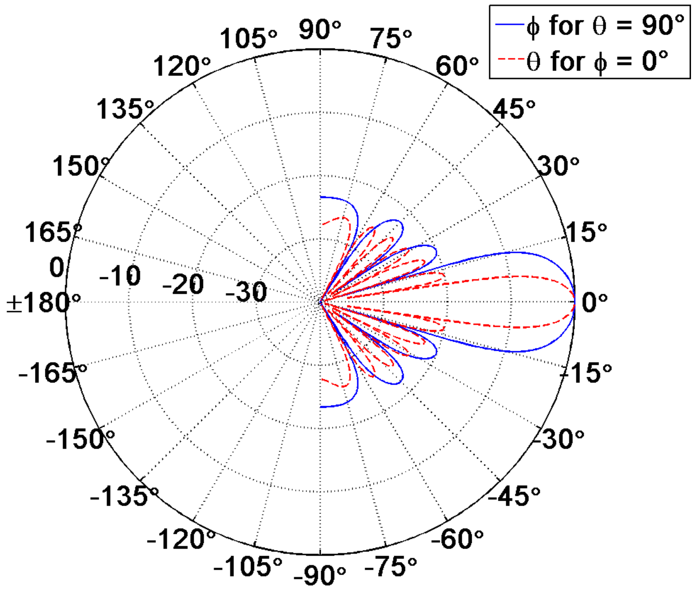
	Receiver	Antenna characteristics: • Gain = 17dBi, • 3dB azimuth width = +/- 12.0°, • 3dB elevation width = +/- 5.0°, • 1st side lobe = -20dBc 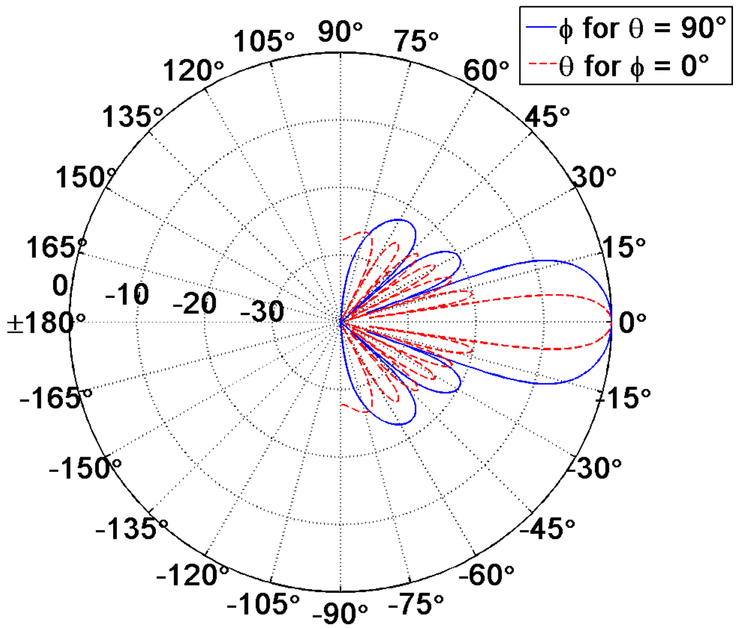 Temperature = 328K, LNA gain = 11.5 dB, LNA noise figure = 6 dB, Mixer gain = 10 dB, Mixer noise figure = 6 dB,

<table>
<tr><td></td><td></td><td>IFA gain = 30 dB,
IFA noise figure = 10 dB,
IF filter bandwidth = 100kHz, 4th order
ADC resolution = 14bit, max input voltage = 3.3V</td></tr>
<tr><td>Interferer: Radar speed meter (RSM) at 24GHz</td><td>Transmitter</td><td>Radar principle: CW (type B1 according to [MT21]),
CW parameters:
Center frequency = 24.15GHz
Transmit power = 20dBm eirp
Antenna characterisitics:
3dB azimuth width = +/- 2.5°,
3dB elevation width = +/- 2.5°,
1st side lobe = -20dBc
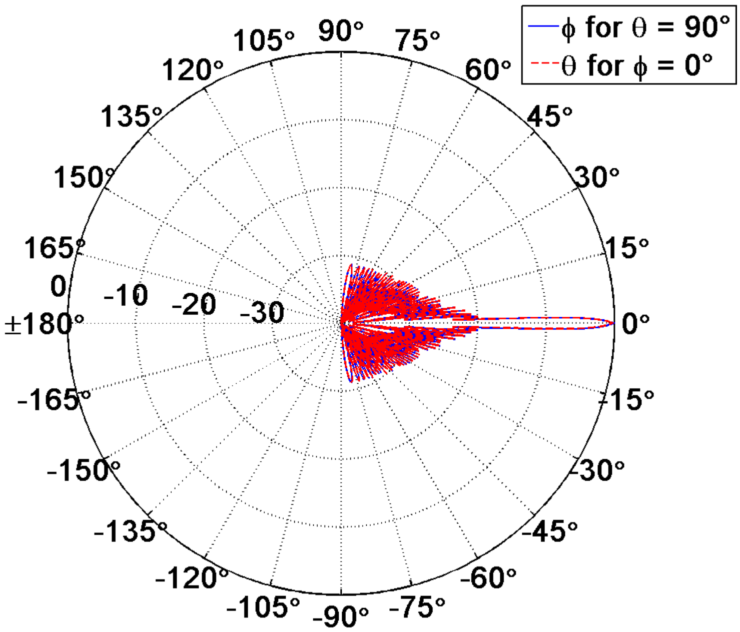
</td></tr>
</table>

Tab. 6.1: Basic parameters used for scenario simulation with CW RSM interferer and FMCW FLR victim at 24GHz.

Now simulations are performed based on parameters out of Tab. 5.

Layer	Receiver Elements	No.	Possible incident	Qualitative interference effect	Quantitative interference effect using M1
Physical	Channel	C1.1	Multipath effects		✓
	Antenna	R1.1			✓
	LNA	R2.1	Driven into compression	Nonlinear distortion	Not occuring
		R2.2	Driven into saturation	Clipping	Not occuring
	Mixer Output	R3.1	Driven into compression	Nonlinear distortion	Not occuring

		R3.2	Driven into saturation	Clipping	Not occuring
	IFA	R4.1	Driven into compression	Nonlinear distortion	Not occuring
		R4.2	Driven into saturation	Clipping	Not occuring
	Active IF filter output	R5.1	Interference with "short" dwell time	Parasitic timely "short" overlayed signal	The time of interference between FMCW and CW is constant, for this paramters 33.3us
		R5.2	Interference with "long" dwell time	Parasitic periodic overlayed signal	Not occuring
		R5.3	Driven to max. supply voltage	Clipping	Not occuring
	ADC output	R6.1	Driven to max. numeric value	Clipping	Not occuring
Raw signal	Pre-filtering	R7.1			
	FFT result	R8.1	See R5.1	Increased noise	Occuring with ca. 5dB (see Fig. 6.2
		R8.2	See R5.2	Single or multiple parasitic peaks	Not occuring
Target	CFAR peak detection (target detection)	R9.1	See R8.1 and R8.2	Increase of adaptive detection level	5dB
		R9.2	See R8.2	Parasitic peaks	Not occurring
	Target property estimation	R10.1			Not yet implemented
Object	Clustering (object detection)	R11.1			Not yet implemented
	Object tracking	R12.1			Not yet implemented

Sensor-Fusion	Logic	R13.1			Not yet implemented
Action	Logic	R14.1			Not yet implemented

Tab. 6.2: Example simulation result for a typical interference scenario (CW interferes FMCW).

Fig. 6.2 shows an increased noise floor in the receiver due to the interference with the RSM. The loss in SNR for a beat frequency of about 20kHz is about 5 dB.

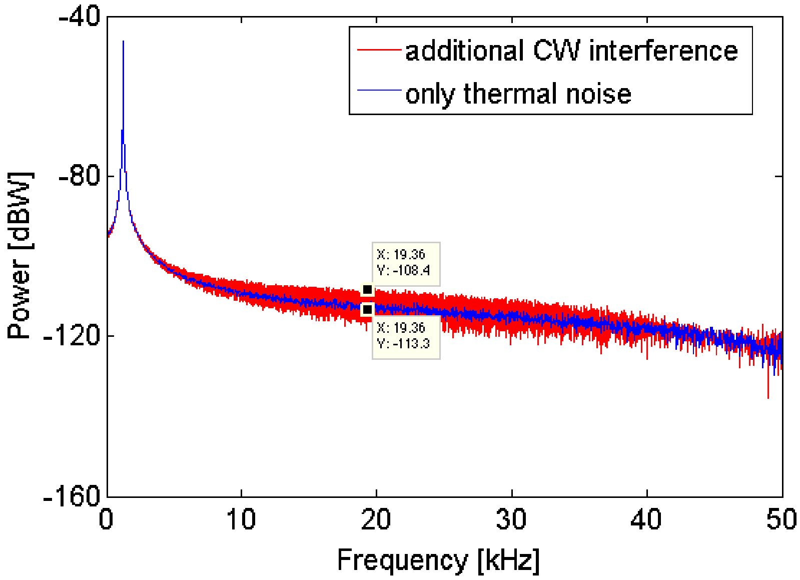

Fig.: 6.2: FMCW radar is interfered by CW road speed meter.

Fig. 6.3 shows the same simulation, but without synthetic target. The result is also an increased noise floor of about 5dB. This can be clearly seen with help of a simple CA-CFAR threshold.

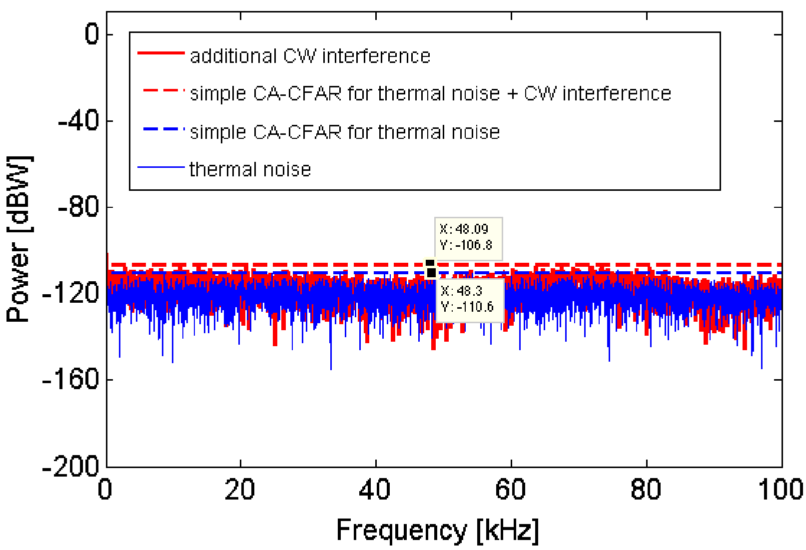

Fig.: 6.3: Interference effect from CW radar when FMCW victim radar has no target in range

6.2. Simulation of ghost target effect

When radar devices detect a target indirectly over reflections within an environment, the radar detects so called "ghost targets".

Ghost targets can be produced by

1) The victim radar itself in environments with a high amount of multi-paths. This is the common case and this is no interference that is directly handled within the MOSARIM project.

2) Other, interfering radars, which have a similar slope to the victim radar. The probability of the occurrence of these types of ghost targets is by far lower than for the ghost targets of type 1), because the slopes have to be quiet the same and the resulting beat frequency has to be within the IF-filter bandwidth. This ghost target effects is an interference effect.

A good scenario to demonstrate the ghost targets described in 1) is a tunnel, see (Fig. 6.4). This 2-lane tunnel cars are placed every 50m for a distance of about 800m. The red dot is the victim transmitter, the green dot is the victim receiver. The victim radar setup is equal to the radar described in Tab. 6.2 and again susceptibility model M1 is used for simulation. No interferer is present in this scenario and all ghost targets are created by the victim radar itself. Only the first peak in Fig. 6.4 corresponds to a direct reflection. All other reflections correspond to multipath effects, because only an orthogonal polygon can lead to a direct reflections (no Lambertian scattering is activated).

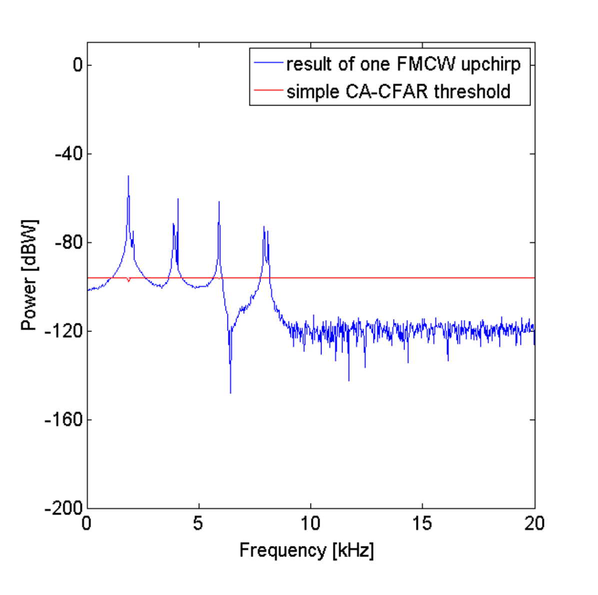

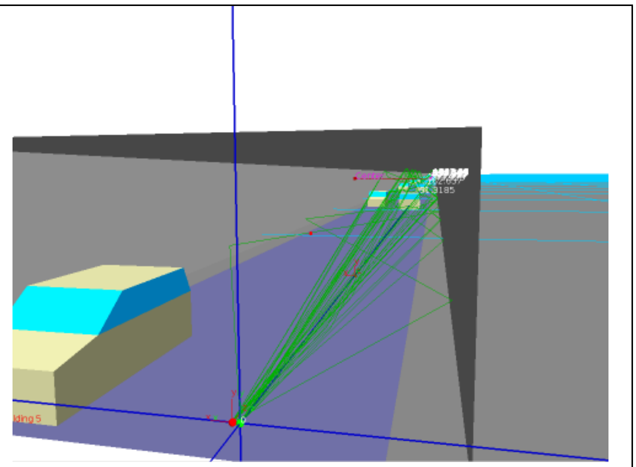

Above: fictive tunnel scenario.
Left: only first peak from the left corresponds to a direct reflection !

Fig. 6.4: Ghost targets as a result of multi path effects in a tunnel.

Also it is possible to draw lines at the known positions of targets. Based on the known target positions, the amount of ghost targets can be assessed and scenarios could be rated regarding their risk to produce ghost targets.

Further simulations will mainly consider type 2) ghost targets.

7. Conclusion and outlook to following tasks of WP2

In this task, the signal modelling and simulation possibilities have been further developed to achieve more detailed and thus better understanding of interference effects.

For the simulation required in coming tasks, the ray-tracing simulation and Matlab signal processing will be further developed with respect to:

- Generic target processing (CFAR)
- Generic object processing (tracking)
- Make simulation output data compatible with practicable signal processing hardware
- Comparison of simulation results with laboratory and real world measurements
- Improved RCS consideration

Also a detailed cross-check of the Matlab signal processing chain with specialized simulation tools like LTSpice or ADS, as well as with measurements is planned.

8. References

[CEPT] *Immunity of 24 GHz automotive SRRS, operating of a non interference and non-protected basis from emissions oft he primary fixed service operating in the 24 GHz and 26 GHz frequency bands* ,ECC report 64, Electronic Communications Committee, 2004

[D13] *Determination and definition of basic radar interference mechanisms, effects and impact on sensor performance and identification of key sensor parameters*, Deliverable 1.3, MOSARIM project (7th EU framework project)

[D17] *Estimation of interference risk from incumbent frequency users and services*, Deliverable 1.7, MOSARIM project (7th EU framework project)

[D41] *Ground truth interference assessment*, Deliverable 4.1, MOSARIM project (7th EU framework project)

[GenDOC] General Document of the MOSARIM project, collects remarkable results and informations.

[MT21] *Establishing of a common interference interaction matrix and evaluation factors*, Milestone document 2.1, MOSARIM project (7th EU framework project)

[1a] Mende, R., *Radarsysteme zur automatischen Abstandsregelung in Automobilen*. Dissertation, TU Braunschweig, 1999.

[1b] Winner, H., Hakuli, S. and Wolf, G., *Handbuch Fahrerassistenzsysteme Grundlagen, Komponenten und Systeme für aktive Sicherheit und Komfort*. Vieweg+Teubner, 2009.

[4a] Born, M. and Wolf, E., *Principles of Optics. Pergamon Press*, Oxford, 2. Edition, 1964.

[4b] Geng,N. and Wiesbeck, W., *Planungsmethoden für die Mobil-kommunikation*, Springer, Berlin, 1998.

[4c] McNamara, D.A., Pistorius, C.W.I., and Malherbe, J.A.G., *Introduction o the Uniform Geometrical Theory of Diffraction*. Artech house, Boston 1990.

[4d] J. Maurer, *Strahlenoptisches Kanalmodell für die Fahrzeug-Fahrzeug Kommunikation.* (in German) PhD thesis, Universität Karlsruhe (TH), May 2005.

[4e] Buddendick, H., Eibert, T., *Simplified Modeling of Complex Shaped*

Objects Using Scattering Center Distributions and Ray Optics. Antennas and Propagation Society International Symposium, San Diego, 2008.

[4f] Computer Simulation Technology, www.cst.com

[4g] 3D Full-wave Electromagnetic Field Simulation, www.ansoft.com

[4h] Schuler, K., Becker, D., and Wiesbeck, W., *Extraction of Virtual Scattering Centers of Vehicles by Ray-Tracing Simulations*. IEEE Transactions on Antennas and Propagation, vol. 56, page 3543 - 3551, Year 2008

9. Abbreviations

A	Amplifier
ADC	Analog Digital Converter
ADS	Advanced Design System (schematic and layout tool from Agilent)
ANT	Antenna
CFAR	Constant False Alarm Rate
CA-CFAR	Cell averaging CFAR
CS	Chirp Sequence (Modulation scheme)
CW	Continuous Wave (Modulation scheme)
dB	Decibel
dBi	dB relative to an isotropic radiator
dBc	dB relative to a main lobe
DSP	Digital Signal Processor
EIRP	Equivalent Isotropic Radiated Power
FDTD	Finite Difference Time Domain
FFT	Fast Fourier Transform
FLR	Forward Looking Radar
FMCW	Frequency Modulated Continuous Wave (Modulation scheme)
FSK	Frequency Shift Keying (Modulation scheme)
GO	Geometrical-Optics
HFA	High Frequency Amplifier
IFA	Intermediate Frequency Amplifier (where intermediate means baseband in this document)
LMFSK	Linear Modulated Frequency Shift Keying (Modulation scheme)
LNA	Low Noise Amplifier
LO	Local Oscillator
LP	Low-pass
PO	Physical Optics
RCS	Radar Cross Section
RSM	road speed meter
RX	Receiver
STL	Standard Triangular Language
TX	Transmitter
UTD	Uniform Theory Diffraction
VCO	Voltage Controlled Oscillator
VW	Volkswagen